

Molybdenum-99 (^{99}Mo) Adsorption Profile of Zirconia-Based Materials for $^{99}\text{Mo}/^{99\text{m}}\text{Tc}$ Generator Application

Marlina^{1*}, E. Lestari¹, Abidin¹, Hambali¹, I. Saptiama^{1,2}, S. Febriana¹, Kadarisman¹, R. Awaludin¹, M. Tanase³, K. Nishikata⁴ and K. Tsuchiya⁴

¹Center for Radioisotopes and Radiopharmaceutical Technology, National Nuclear Energy Agency (BATAN), Puspiptek Area Serpong, Tangerang Selatan 15314, Indonesia

²Faculty of Medicine, University of Tsukuba, 1-1-1 Tennoudai, Tsukuba, Ibaraki 305-8576, Japan

³Oarai Research Center, Chiyoda Technol Corporation, Oarai, Ibaraki 311-1133, Japan

⁴Oarai Research and Development Institute, Japan Atomic Energy Agency, Oarai, Ibaraki 311-1393, Japan

ARTICLE INFO

Article history:

Received 3 December 2018

Received in revised form 13 November 2019

Accepted 23 March 2020

Keywords:

Low specific activity

Zirconia

Adsorption capacity

$^{99}\text{Mo}/^{99\text{m}}\text{Tc}$ generator

ABSTRACT

Technetium-99m ($^{99\text{m}}\text{Tc}$) plays a major role in diagnostic nuclear medicine and has not yet been replaced with any other radionuclides. It is available through the $^{99}\text{Mo}/^{99\text{m}}\text{Tc}$ generator. The use of low-specific-activity ^{99}Mo for $^{99}\text{Mo}/^{99\text{m}}\text{Tc}$ generator application requires high adsorptive capacity sorbents. This study focused on the determination of ^{99}Mo adsorption capacity of several zirconia materials, namely monoclinic nanozirconia, orthorhombic nanozirconia, sulfated zirconia, and phosphated zirconia. These materials were synthesized by using the sol-gel method and characterized using FT-IR spectroscopy, X-ray diffraction (XRD), and scanning electron microscopy/energy-dispersive X-ray spectroscopy (SEM-EDS). The determination of ^{99}Mo adsorption capacity of these materials was carried out by soaking the materials in a $\text{Na}_2^{99}\text{MoO}_4$ solution with pH of 3 and 7, at temperatures ranging from room temperature to 90 °C, for 1 and 3 hours. The results indicated that monoclinic nanozirconia has a ^{99}Mo adsorption capacity of 76.9 mg Mo/g, whereas orthorhombic nanozirconia, sulfated zirconia, and phosphated zirconia have ^{99}Mo adsorption capacities of 150.1 mg Mo/g, 15.58 mg Mo/g, and 12.74 mg Mo/g, respectively. It appears that orthorhombic nanozirconia has the highest ^{99}Mo adsorption capacity among the synthesized materials and can be applied as a candidate material for the $^{99}\text{Mo}/^{99\text{m}}\text{Tc}$ generator.

© 2020 Atom Indonesia. All rights reserved

INTRODUCTION

Technetium-99m ($^{99\text{m}}\text{Tc}$) plays a major role in diagnostic nuclear medicine for approximately 80-85 % of all nuclear medicine procedures and has not yet been replaced with any other radionuclides [1-3]. The $^{99\text{m}}\text{Tc}$ ($t_{1/2} = 6$ h; 140 keV), the daughter radionuclide of Molybdenum-99 (^{99}Mo) through beta (β^-) decay, is the most widely used radioisotope for diagnostic radiopharmaceuticals in nuclear medicine [4]. The $^{99\text{m}}\text{Tc}$ -radiopharmaceuticals are primarily used in the study of some organs system. For instance, $^{99\text{m}}\text{Tc}$ -sestamibi, $^{99\text{m}}\text{Tc}$ -tetrafosmin, and $^{99\text{m}}\text{Tc}$ -teboroxime are used to diagnosis of heart, while $^{99\text{m}}\text{Tc}$ -DTPA is used to measure the

glomerular filtration rate in the kidney. For liver diagnostic, $^{99\text{m}}\text{Tc}$ -lidofenin is used, while $^{99\text{m}}\text{Tc}$ -medronate and $^{99\text{m}}\text{Tc}$ -xydronate are used for skeletal imaging, whereas $^{99\text{m}}\text{Tc}$ -propyleneamineoxime is used as a cerebral perfusion agent [5,6].

The $^{99\text{m}}\text{Tc}$ is available through $^{99}\text{Mo}/^{99\text{m}}\text{Tc}$ generators. Over 95 % of the ^{99}Mo required for $^{99\text{m}}\text{Tc}$ generators is produced by the fission of ^{235}U targets in nuclear research reactors [7,8]. This fission reaction results in a high specific activity of ^{99}Mo ($>10^4$ Ci/g Mo). The $^{99\text{m}}\text{Tc}$ generators based on the high specific activity of ^{99}Mo commonly use alumina as an adsorbent for generator column.

Several $^{99}\text{Mo}/^{99\text{m}}\text{Tc}$ generators are commercially available, such as Ultra-Technekow V4 from Curium and similar products from POLATOM and ANSTO. Recently, unstable supply

*Corresponding author.

E-mail address: marlina@batan.go.id

DOI: <https://doi.org/10.17146/aij.2020.914>

of ^{99}Mo due to uranium restriction and reactor aging problems is a global issue [9,10]. Therefore, it is necessary to develop an alternative technology in $^{99}\text{Mo}/^{99\text{m}}\text{Tc}$ generator preparation to face that problem.

Low-specific-activity ^{99}Mo (<10 Ci/g of molybdenum) can be produced by neutron activation of natural or enriched ^{98}Mo in a nuclear research reactor, by gamma irradiation of ^{100}Mo in accelerator facility, and by charged-particle activation of ^{100}Mo in cyclotron facility [11-14]. The achievable low specific activity of ^{99}Mo so produced is less favorable, but the absolute amounts can be sufficient for local needs [10]. For $^{99}\text{Mo}/^{99\text{m}}\text{Tc}$ generator application, low-specific-activity ^{99}Mo could not be adsorbed to the alumina adsorbent, due to the limited adsorption capacity of alumina to molybdenum; however, it has to be adsorbed by high capacity adsorbents. Recently, nanomaterial-based adsorbents appear to have a promising prospect as high capacity adsorbents due to their physical properties. The small particle size of nanomaterial adsorbents can increase its surface energy and adsorption capacity to metal ions [15].

Several nanomaterial adsorbents have been developed for $^{99}\text{Mo}/^{99\text{m}}\text{Tc}$ generator application, namely polymer-embedded nanocrystalline titania, tetragonal nanocrystalline zirconia, and nanocrystalline alumina [15-17].

This study focused on the determination of ^{99}Mo adsorption capacity of some zirconia materials which have been synthesized in previous work [18], namely monoclinic nanozirconia and orthorhombic nanozirconia, as well as sulfated zirconia and phosphated zirconia whose synthesis processes are reported in this report.

The introduction of anionic groups (e.g., sulfate, phosphate) at the surface of metal oxides markedly enhances its acidic properties [19]. Thus, it is expected to improve Mo adsorption capacity of zirconia materials.

Sulfated zirconia was used as a catalyst for organic transformations due to its strong acidic properties, especially for developing environmentally friendly processes in alkane isomerization at mild temperature [20] as well as for hydrocarbon isomerization, alkylation, and esterification [21].

EXPERIMENTAL METHODS

Reagents including $\text{ZrOCl}_2 \cdot 8\text{H}_2\text{O}$, isopropyl alcohol, ammonia 32 %, pH-indicator strips pH 0-14 universal indicator, sulfuric acid, and phosphoric acid was purchased from Merck, while water and

demineralized water were purchased from a local company, IPHA, Bandung, Indonesia. Molybdenum trioxide was purchased from Sigma-Aldrich. All reagents used were analytical grade.

The equipment used consisted of beaker glasses, hot plate stirrers, evaporating dishes, thermometers, a furnace (Raypa), an Alpha FT-IR spectrometer (Bruker), and a Miniflex 600 X-Ray diffractometer (Rigaku). Characterization was carried out using the spectrometer. The spectra were recorded in the range of $450\text{-}4000\text{ cm}^{-1}$.

Preparation of $\text{Na}_2^{99}\text{MoO}_4$ solution

To produce ^{99}Mo via $^{98}\text{Mo}(n,\gamma)$ reaction, a total of 4 grams of natural molybdenum trioxide (MoO_3) was irradiated in the G. A. Siwabessy nuclear reactor, BATAN, Serpong, Indonesia. The irradiation was carried out at reactor power of 15 MW and neutron flux of $1.3 \times 10^{14}\text{ n cm}^{-2}\text{ s}^{-1}$ for 5 days. After irradiation process, the MoO_3 target was dissolved using 4 M sodium hydroxide solution. This process resulted in a ^{99}Mo solution with a specific activity of 0.3-0.5 Ci/g Mo. All work was carried out in a hot cell facility. ^{99}Mo solutions of pH 3 and 7 were prepared by adding 6 M HCl to the bulk of the ^{99}Mo solution. The radioactivity of the ^{99}Mo solutions was measured by using a dose calibrator (Atomlab 100Plus).

Synthesis of monoclinic nanozirconia and orthorhombic nanozirconia

Monoclinic nanozirconia and orthorhombic nanozirconia were synthesized based on the method described in our previous works [18].

Synthesis of sulfated zirconia

Zirconium solution was prepared by dissolving $\text{ZrOCl}_2 \cdot 8\text{H}_2\text{O}$ in 80 % isopropyl alcohol. Then, 20 % ammonium solution in isopropyl alcohol was added to the zirconium solution. The mixture was strongly stirred without heat until a white gel was formed. The mixture keeps stirred for 14 hours. The filtrate was separated, then the gel was washed with 80 % 2-propanol solution until free of Cl^- ion. Then, 40 mL of 0.5 M sulfuric acid solution was added to the gel. The mixture was refluxed for 12 hours at $95\text{ }^\circ\text{C}$. The gel was transferred into the evaporating dish and then heated at $110\text{ }^\circ\text{C}$ to dry the precipitate. The precipitate was calcined at $600\text{ }^\circ\text{C}$ for 2 hours. The white solid formed was sieved in the size of 50-100 mesh.

Synthesis of ppphosphated zirconia

The phosphated zirconia was synthesized by using a similar procedure to sulfated zirconia, but the sulfuric acid in the synthesis of sulfated zirconia was replaced by phosphoric acid. The mixture was refluxed for 6 hours at 110 °C.

Characterization of synthesized materials

The characterization of the materials was carried out by using Fourier transform infrared spectroscopy using the Alpha FT-IR spectrometer, scanning electron microscopy/energy-dispersive X-ray spectroscopy (SEM-EDS), and powder X-ray diffraction (XRD) using the Miniflex 600 X-ray diffractometer.

Determination of ⁹⁹Mo absorption capacity

Determination of ⁹⁹Mo absorption capacity of the synthesized zirconia materials was performed using the Na₂⁹⁹MoO₄ solution of pH 3 and 7. A total of 100 mg of zirconia, each inserted into 4 tubes containing 0.001 M HNO₃ solution and left for 1 h at room temperature. The filtrate was removed by decantation. A 1 mL portion of the ⁹⁹Mo solution (pH 3 or 7) was added to the zirconia material. The zirconia material was immersed under the conditions specified in Table 1. In this work, the as-synthesized zirconia-based material products were denoted as monoclinic nanozirconia (MZ), orthorhombic nanozirconia (OZ), sulfated zirconia (SZ), and phosphate zirconia (PZ). The filtrate was separated then the precipitate was washed with 500 µL of water. The filtrate and the water were collected and then the radioactivity of ⁹⁹Mo was measured by using dose calibrator.

Table 1. The condition of the zirconia-based material adsorption in ⁹⁹Mo solution.

Tube	Treatment duration (hours)	Temperature
1	1	Room temperature
2	3	Room temperature
3	1	90 °C
4	3	90 °C

RESULTS AND DISCUSSION

Monoclinic nanozirconia and orthorhombic nanozirconia

The synthesis and characterization of monoclinic nanozirconia and orthorhombic nanozirconia were discussed in our previous work [18].

Sulfated zirconia

The synthesized sulfated zirconia is shown in Fig. 1. The sulfated zirconia prior to calcination is a light yellow solid. After calcination, its color turns white.



Fig. 1. The sulfated zirconia: (a) prior to calcination (b) after calcination.

The FTIR spectra of sulfated zirconia are shown in Fig. 2. Figure 2a shows the FT-IR spectrum of sulfated zirconia prior to calcination. The absorption peaks at 3283 and 1635 cm⁻¹ are attributed to the stretching and bending vibrations of the OH groups of the water. These absorption peaks disappeared after calcination at 600 °C (Fig. 2b). The absorption peaks at 450-600 cm⁻¹ show the presence of a Zr-O-Zr group (Figs. 2a and 2b). The absorption peak at 900-1200 cm⁻¹ is attributed to the S=O and S-O groups, which is typical for bidentate sulfate groups with inorganic chelates [22].

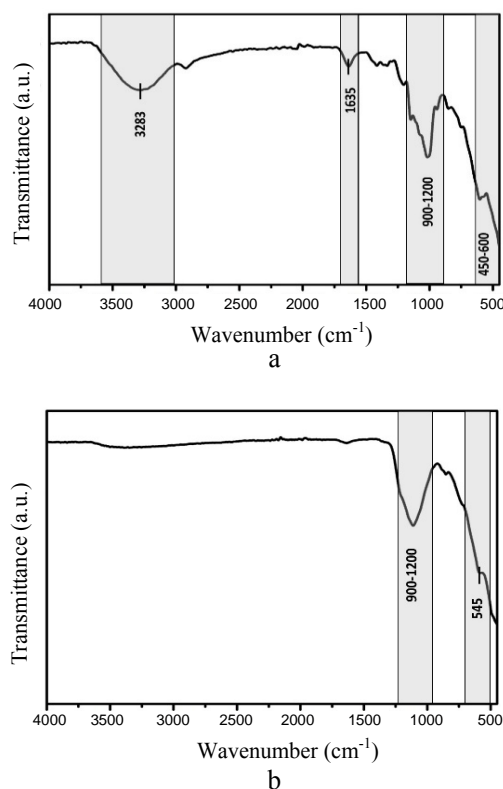


Fig. 2. The FTIR spectra of sulfated zirconia: (a) prior to calcination (b) after calcination.

The SEM image of the synthesized sulfated zirconia shows that the particles have a sphere-like shape (Fig. 3). The composition of elements in the surface of synthesized sulfated zirconia and its energy is shown in Table 2. Based on the SEM-EDX measurements (Fig. 4), the presence of S element indicates that sulfated zirconia has been formed.

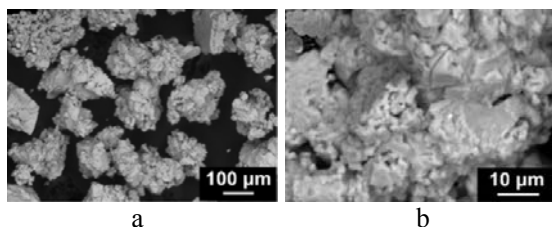


Fig. 3. The SEM images of synthesized sulfated zirconia: (a) low and (b) high magnification.

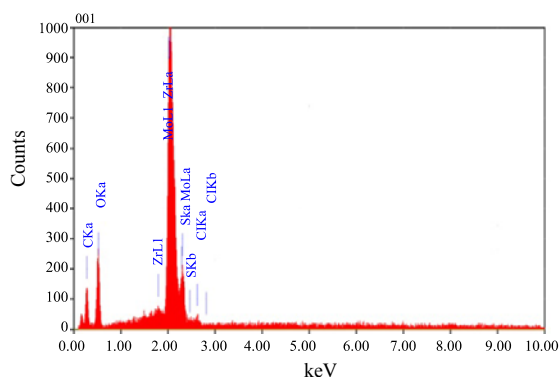


Fig. 4. EDS spectrum of the synthesized sulfated zirconia.

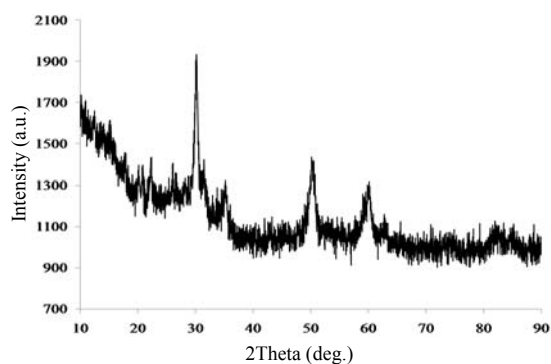


Fig. 5. The XRD pattern of the synthesized sulfated zirconia.

Table 2. The composition of elements in the surface of the synthesized sulfated zirconia.

	Energy (keV)	% Mass
Carbon (C)	0.277	24.79
Oxygen (O)	0.525	29.10
Sulfur (S)	2.307	2.46
Chlorine (Cl)	2.621	0.43
Zirconium (Zr)	2.042	38.41
Molybdenum (Mo)	2.293	4.80

The XRD analysis result of the synthesized sulfated zirconia is shown in Fig. 5. The crystal peaks at $2\theta = 30.1^\circ, 34.9^\circ, 50.1^\circ,$ and 59.7° are the characteristic peaks for sulfated zirconia with tetragonal crystal [22,23].

Phosphated zirconia

The FTIR spectra of synthesized phosphated zirconia are shown in Fig. 6. Figure 6a shows the FTIR spectrum of synthesized phosphated zirconia prior to calcination. The absorption peaks at 3139 and 1616 cm^{-1} are attributed to the stretching and bending vibration of OH groups of the water. These absorption peaks disappeared after calcination at $600\text{ }^\circ\text{C}$ (Fig. 6b). The absorption peaks at $900\text{-}1200\text{ cm}^{-1}$ show the presence of P-Zr-O groups (Figs. 6a and 6b). The absorption peak at 495 cm^{-1} (Fig. 6a) is attributed to the Zr-O group that shifts to the wave number of 545 cm^{-1} after calcination (Fig. 6b) [19].

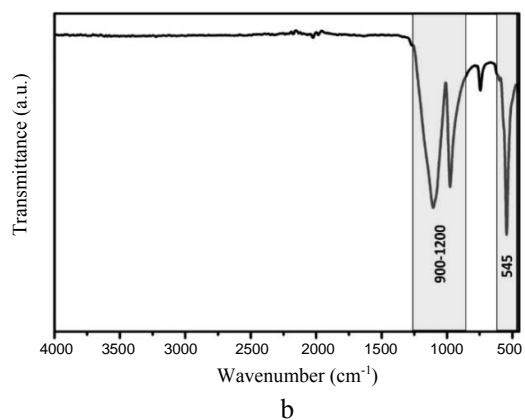
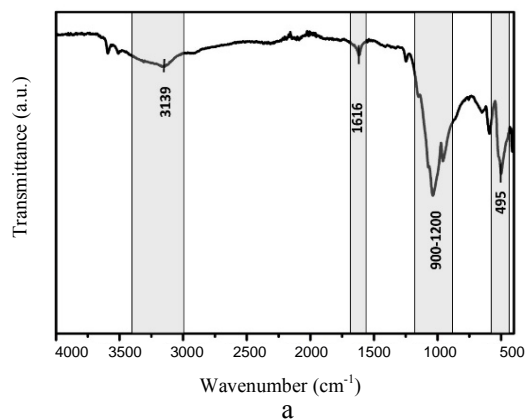


Fig. 6. The FTIR spectra of phosphated zirconia: (a) before calcination (b) after calcination.

The SEM image of the synthesized phosphated zirconia shows that the material has a

sphere-like shape (Fig. 7). The composition of elements in the surface of the synthesized phosphated zirconia and its energy is shown in Table 3. Based on the SEM-EDX measurements (Fig. 8), the presence of phosphorus indicates that phosphated zirconia has been formed.

Table 3. The composition of elements in the surface of the synthesized phosphated zirconia

Element	Energy (keV)	% Mass
Carbon (C)	0.277	28.41
Oxygen (O)	0.525	34.72
Phosphor (P)	2.013	20.33
Copper (Cu)	8.040	1.51
Zirconium (Zr)	2.042	15.03

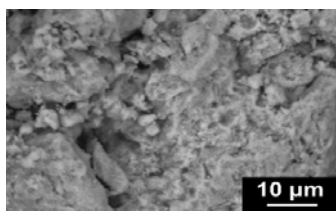


Fig. 7. The high-magnification of SEM image of the synthesized phosphated zirconia.

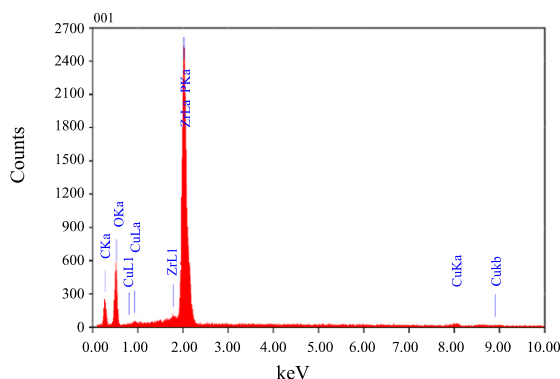


Fig. 8. EDS spectrum of the synthesized phosphated zirconia.

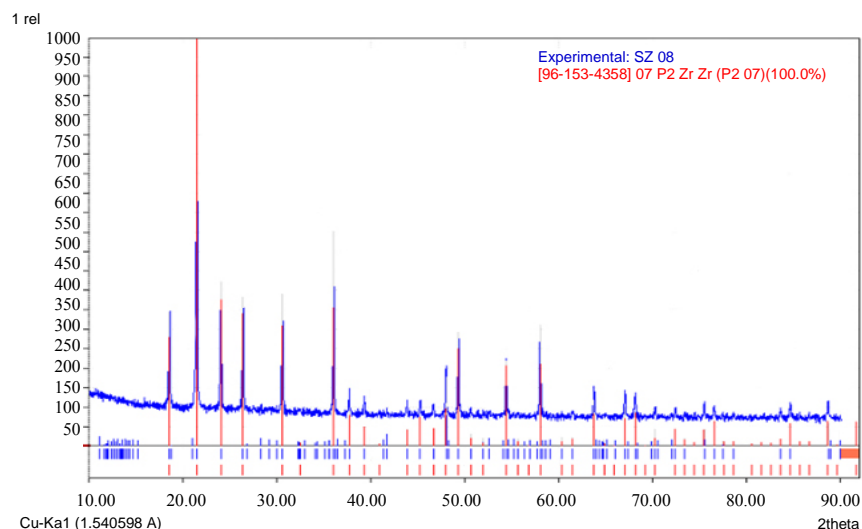


Fig. 9. The XRD pattern of the synthesized phosphated zirconia.

The XRD analysis of the synthesized phosphated zirconia was compared to the database in the Match software package, and a 100 % similarity with the $Zr_2P_2O_7$ was found. The comparison of X-ray diffraction patterns between the synthesized phosphated zirconia and the $Zr_2P_2O_7$ compound is shown in Fig. 9. Based on Fig. 9, there are peaks at $2\theta = 18.63^\circ, 21.55^\circ, 24.12^\circ, 26.47^\circ, 30.66^\circ, 36.12^\circ, 37.78^\circ, 39.39^\circ, 43.92^\circ, 45.32^\circ, 48.08^\circ, 49.41^\circ, 54.49^\circ, 58.11^\circ, 63.84^\circ, 67.13^\circ,$ and 68.22° . These peaks are characteristic for phosphated zirconia with orthorhombic crystals.

The ^{99}Mo adsorption capacities of the synthesized materials

The ^{99}Mo adsorption capacity of the MZ, OZ, SZ, and PZ are shown in Table 4. The MZ has its highest ^{99}Mo adsorption capacity of 76.9 mg Mo/g under the adsorption condition of ^{99}Mo solution of pH = 3, at the temperature of 90 °C for 3 hours. On the other hand, the OZ has its highest ^{99}Mo adsorption capacity of 150.14 mg Mo/g which was obtained under the adsorption condition of ^{99}Mo solution of pH = 3, at the temperature of 90 °C for 1 hour. Orthorhombic zirconia has a smaller crystallite size than other crystalline zirconia [18], and therefore its surface area is much higher than others [24]. Therefore, orthorhombic zirconia belongs to the highest Mo adsorption capacity.

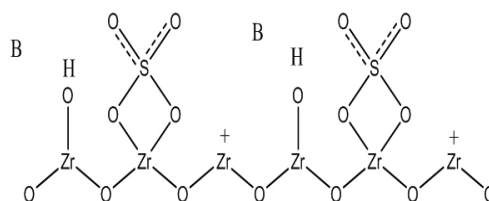
The sulfated zirconia has its highest ^{99}Mo adsorption capacity of 15.58 mg Mo/g as obtained under the adsorption condition of ^{99}Mo solution of pH = 7, at the temperature of 90 °C for 3 hours. In the ^{99}Mo solution of pH = 3 at room temperature, the filtrate of sulfated zirconia becomes turbid during submersion.

Table 4. The profile of ^{99}Mo adsorption capacity of the zirconia-based material.

Adsorbents	Adsorption time	pH of Mo-99 solution = 3		pH of Mo-99 solution = 7	
		^{99}Mo adsorption capacity at room temperature (mg Mo/g)	^{99}Mo adsorption capacity at 90 °C (mg Mo/g)	^{99}Mo adsorption capacity at room temperature (mg Mo/g)	^{99}Mo adsorption capacity at 90 °C (mg Mo/g)
MZ	1 h	55.43	73.77	9.84	20.44
	3 h	54.98	76.9	11.24	20.28
OZ	1 h	100.56	150.14	22.28	40.70
	3 h	98.47	129.11	21.43	36.27
SZ	1 h	11.24	-	5.76	13.22
	3 h	13.15	-	6.65	15.58
PZ	1 h	2.94	5.09	0.92	3.50
	3 h	12.74	10.23	2.00	4.56

Nevertheless, the solid and filtrate could still be separated by decantation. In the ^{99}Mo solution of pH = 3 at the temperature of 90 °C, the sulfated zirconia was suspended in the ^{99}Mo solution. The solid and the filtrate could not be separated. Therefore, both the activity of the solid and filtrate could not be measured, and therefore the absorption capacity of the sulfated zirconia at this temperature cannot be determined. The highest ^{99}Mo absorption capacity of the phosphated zirconia (12.74 mg Mo/g) was obtained under adsorption conditions at room temperature for 3 hours in the ^{99}Mo solution of pH = 3.

In this study, it appears that the introduction of sulfate and phosphate groups onto the surface of zirconia material does not improve the adsorption capacity of molybdenum compared to monoclinic/orthorhombic zirconia. The surface of sulfated zirconia contains very strong Brønsted as well as Lewis acid sites. These sites resulted from the weakening of the O-H bond from adjacent sulfate groups, whereas the Lewis acid sites are electronically deficient Zr^{4+} centers as a result of the electron-withdrawing nature of the sulfate group [25]. The presence of Brønsted and Lewis acid sites is shown in the Fig. 10. Reddy *et al.* [25] have measured the X-ray photoelectron spectroscopy (XPS) intensities of bonding energies of sulfated zirconia as well as of molybdate-zirconia; it was found that the sulfate ion strongly interacts with the support surface followed by molybdate. Sulfate ions exhibits a stronger bond to zirconia (ZrO_2) than do molybdate ions. Consequently, the sulfate ion of the sulfated zirconia cannot be substituted by the molybdate ion. The same phenomena occurs on the phosphated zirconia. Therefore, the Mo adsorption capacity of sulfated and phosphated zirconia become very low, namely 15.58 and 12.74 mg Mo/g, respectively.

**Fig. 10.** The sulfated zirconia structure. The label B signifies Brønsted acid site and Zr^+ is Lewis acid site.

The zirconium materials that have been applied for $^{99}\text{Mo}/^{99\text{m}}\text{Tc}$ generator are PZC (polymeric zirconium compound) and ZBM (zirconium-based material). PZC has a ^{99}Mo adsorption capacity of ~250 mg Mo/g PZC [26], and the ZBM (zirconium-based material) has a ^{99}Mo adsorption capacity of 177-193 mg Mo/g ZBM [13,27]. These materials have been developed by Center for Radioisotopes and Radiopharmaceutical Technology, BATAN, in collaboration with Japan Atomic Energy Agency (JAEA), Kaken Co., Japan, and Chiyoda Technol Corporation, Japan [26-28]. Another zirconia material, tetragonal ZrO_2 (t- ZrO_2), has been reported as having a ^{99}Mo adsorption capacity of 250 mg Mo/g [15]. Also, orthorhombic nanozirconia compounds exhibits a ^{99}Mo adsorption capacity of 150.1 mg Mo/g. It is expected to be an alternative material as an adsorbent for the $^{99}\text{Mo}/^{99\text{m}}\text{Tc}$ generator.

CONCLUSION

In the present study, the synthesized monoclinic nanozirconia has a ^{99}Mo adsorption capacity of 76.9 mg Mo/g, whereas orthorhombic nanozirconia, sulfated zirconia, and phosphated zirconia have ^{99}Mo adsorption capacity of 150.1 mg Mo/g, 15.58 mg Mo/g, and 12.74 mg Mo/g,

respectively. It appears that orthorhombic nanozirconia has the highest ^{99}Mo adsorption capacity among the synthesized materials. Therefore, the orthorhombic nanozirconia is expected to be applied as an alternative candidate material for the $^{99}\text{Mo}/^{99\text{m}}\text{Tc}$ generator.

ACKNOWLEDGMENT

This work is supported by the Indonesian government funding through the National Nuclear Energy Agency, BATAN, as well as the International Atomic Energy Agency (IAEA) Coordinated Research Project F22068 (IAEA Research Contract No. 21033). The authors would like to thank E. Sarmini, Herlina, and Sriyono for technical assistances.

REFERENCES

1. L.M. Filzen, L.R. Ellingson, A.M. Paulsen *et al.*, J. Nucl. Med. Technol. **45** (2017) 1.
2. T.M. Sakr, M.F. Nawar, T.W. Fasih *et al.*, Appl. Radiat. Isot. **129** (2017) 67.
3. M. Amin, M.A. El-Amir, H.E. Ramadan *et al.*, J. Radioanal. Nucl. Chem. **318** (2018) 915.
4. P.H. Liem, H.N. Tran, T.M. Sembiring, Prog. Nucl. Energy **82** (2015) 191.
5. W.C. Eckelman, A.G. Jones, A. Duatti *et al.*, Drug Discov. Today **18** (2013) 984.
6. G.J. Stasiuk, P.M. Holloway, C. Rivas *et al.*, Dalton Trans. **44** (2015) 4986.
7. W.L. Araujo and T.P.R. Campos, Nucl. Inst. Methods Phys. Res. A **782** (2015) 40.
8. J. Welsh, C.I. Bigles and A. Valderrabano, J. Radioanal. Nucl. Chem. **305** (2015) 9.
9. T. Takeda, M. Fujiwara, M. Kurosawa *et al.*, J. Radioanal. Nucl. Chem. **318** (2018) 811.
10. M. Blaauw, D. Ridikas, S. Baytelesov *et al.*, J. Radioanal. Nucl. Chem. **311** (2017) 409.
11. P. Martini, A. Boschi, G. Cicoria *et al.*, Appl. Radiat. Isot. **118** (2016) 302.
12. T.J. Ruth, J. Nucl. Med. Technol. **42** (2014) 245.
13. I. Saptiama, E. Lestari, E. Sarmini *et al.*, Atom Indonesia **42** (2016) 115.
14. S.K. Lee, G.J. Beyer and J.S. Lee, Nucl. Eng. Technol. **48** (2016) 613.
15. R. Chakravarty and A. Dash, J. Radioanal. Nucl. Chem. **299** (2014) 741.
16. I. Saptiama, Y.V. Kaneti, Y. Suzuki *et al.*, Small **14** (2018) 1800474.
17. Kadarisman, Sriyono, Abidin *et al.*, Atom Indonesia **44** (2018) 17.
18. Marlina, E. Sarmini, Herlina *et al.*, Atom Indonesia **43** (2017) 1.
19. G.A.H. Mekhemer, Colloids Surf. A: Physicochem. Eng. Asp. **141** (1998) 227.
20. K. Saravanana, B. Tyagia and H. Bajaja, Indian J. Chem. **53** (2014) 799.
21. M. Ejtemaei, A. Tavakoli, N. Charchi *et al.*, Adv. Powder Technol. **25** (2014) 840.
22. M.K. Mishra, B. Tyagi and R.V. Jasra, J. Mol. Catal. A: Chem. **223** (2004) 61.
23. F. Heshmatpour and R.B. Aghakhanpour, Adv. Powder Technol. **23** (2012) 80.
24. K.J.A. Raj and B. Viswanathan, Indian J. Chem. **48A** (2009) 1378.
25. B.M. Reddy, P.M. Sreekanth, Y. Yamada *et al.*, Appl. Catal. A: Gen. **228** (2002) 269.
26. H. Adang, A. Mutalib, H. Lubis *et al.*, Proceeding of National Conference on Basic Research and Nuclear Technology, BATAN, (2011) 44. (in Indonesian)
27. I. Saptiama, Marlina, E. Sarmini *et al.*, Atom Indonesia **41** (2015) 103.
28. R. Awaludin, A.H. Gunawan, H. Lubis *et al.*, J. Radioanal. Nucl. Chem. **303** (2015) 1481.